Memorylike response of the magnetic glass

Sudip Pal, Kranti Kumar, and A. Banerjee
UGC-DAE Consortium for Scientific Research, University Campus, Khandwa Road, Indore-452001, India

(Received 18 November 2020; revised 17 February 2021; accepted 6 April 2021; published 27 April 2021)

Nonergodicity of phase coexisting state is not trivial, and its understanding is yet unclear. We have investigated two prototype manganites, $Pr_{0.5}Ca_{0.5}Mn_{0.975}Al_{0.025}O_3$ and $La_{0.5}Ca_{0.5}MnO_3$ where ferromagnetic and antiferromagnetic phases coexist at low temperatures due to kinetic arrest of a first-order transition. We have studied the evolution of the dynamics of a kinetically arrested state with temperature and magnetic field. We also highlight a peculiar nonequilibrium behavior of the phase coexisting state that appears like the memory effect, which basically is an intrinsic property of spin glasses or related systems. If the volume fraction of the two coexisting phases is altered by changing magnetic field at a temperature T_m during cooling, the phase fraction is fully or partially reacquired during heating above T_m depending on which phase among the coexisting phases is the actual equilibrium phase of the system. We suggest that the memorylike response observed here is not due to competing exchange interaction, instead arises due to supercooling, superheating, and kinetic arrest of the associated transition. Such magnetic response provides an easy method of identifying the ground state of a kinetically arrested system.

DOI: 10.1103/PhysRevB.103.144434

I. INTRODUCTION

Memory effect is a well known phenomenon in spin glass and similar systems, being studied in physics and biology [1–4]. It brings out the system's unique tendency to remember and recall it's history. It arises due to rugged potential energy landscape consisting of copious metastable energy basins [5–7]. A heterogeneous phase coexisting state where competing magnetic phases coexist in spatially separated regions often show nonequilibrium responses, including the memory effect and have been described as the spin glass, cluster glass, re-entrant spin-glass-like states, etc. essentially arising due to competing interactions [8–11]. It has been proposed earlier that the phase coexistence can also appear due to kinetic arrest of a first-order magnetic transition [12–15]. In such materials, two long-range magnetic states (for example, antiferromagnetic, ferromagnetic, etc.) are separated by a first-order transition in magnetic field (H) - temperature (T) plane. Yet, the two phases coexist down to the lowest temperature because the transition fails to complete in a certain H-T window. It is called as the kinetic arrest of the transition and the low temperature state is named as the magnetic glass (MG) because it shows nonequilibrium behavior. Nonetheless, MG is fundamentally different from a spin glass, re-entrant spin glass or cluster glass [16–18]. Truly, the present understanding of glasses is not so transparent and hence their seemingly identical bulk responses are often interpreted injudiciously. In this light, we study two prototype systems, $Pr_{0.5}Ca_{0.5}Mn_{0.975}Al_{0.025}O_3$ (PCMAO) and $La_{0.5}Ca_{0.5}MnO_3$ (LCMO), where the formation of MG is reported earlier. We shall highlight some atypical nonequilibrium responses of the MGs. We reveal an intriguing memorylike effect and explain it in the framework of the supercooling, superheating, and kinetic arrest of a first-order phase transition.

Growing number of evidences of arrested first-order transitions across various magnetostructural transitions, metal-insulator transitions, in multiferroics, etc. has turned it into an important aspect in the phase diagram [19–26] and promise practical applications [27]. Usually, a first-order magnetic transition in H-T plane is dictated by the presence of supercooling (H^*, T^*) and superheating (H^{**}, T^{**}) lines, which are instrumental only during cooling and heating, respectively [28]. Accordingly, the transition shows thermal hysteresis in physical properties while measured in the cooling and heating cycles. At the transition temperature (T_C), two phases (high- and low-T phases) coexist and remain separated by a free energy barrier. As T decreases, the free energy barrier reduces till T^* and in the intermediate temperature range, i.e., $T^* < T < T_C$, high-T phase can still persist, trapped at a local minima, as a metastable state. However, below (H^*, T^*), the high-T phase spontaneously transforms to the low-T phase. Additionally, a kinetic arrest line (H_K, T_K) has been proposed to also play important role besides (H^*, T^*) and (H^{**}, T^{**}) lines [12,13,29]. The role of (H_K, T_K) is, if during cooling T_K appears above T^*, the high-T to low-T phase transition is arrested below T_K and the T^* laying below T_K becomes ineffective. The high-T phase then persists even below (H^*, T^*) as a glasslike state. This arrested state undergoes devitrification, i.e., transforms to the equilibrium phase while heating above the T_K line, which is essentially akin to the structural glass.

However, practically, presence of quenched disorder broadens (H^*, T^*), (H^{**}, T^{**}), and (H_K, T_K) lines into bands i.e., the transition temperatures are distributed in a wide H-T landscape [13,30]. In Figs. 1(a) and 1(b), we have shown the phenomenological band diagrams for two different kind of systems which have the ferromagnetic (FM) and antiferromagnetic (AFM) low-T states, respectively [31]. We have shown only (H^*, T^*) and (H_K, T_K) bands because these two

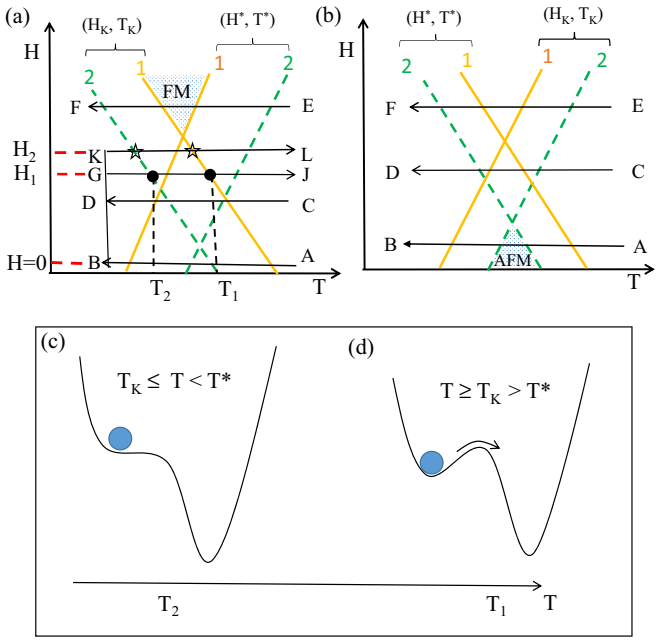

FIG. 1. Phenomenological (H^*, T^*) and (H_K, T_K) bands explaining kinetic arrest in systems having (a) FM as equilibrium low-T phase and (b) AFM as equilibrium low-T phase. Each band is drawn for two different regions in the sample. In both schematics, (H^*, T^*) and (H_K, T_K) are anticorrelated, i.e., if region 1 (R1) has lower T^* than region 2 (R2), then, R1 has higher T_K compared to R2 as in (a) or vice versa. (c) Schematic of free energy in the temperature range $T_K \leqslant T < T^*$ and (d) in the temperature range $T \geqslant T_K > T^*$.

bands are important during cooling at a constant magnetic field. In both of these figures, one should notice three crucial points. First, each band has been drawn consisting of only two parallel lines for simplicity, which represent different transition temperatures of two different regions in the sample. This is due to broadening and in principle consist of continuum of lines forming bands. Second, (H^*, T^*) and (H_K, T_K) bands are anticorrelated, i.e., a region that has higher T^*, also has relatively lower T_K [31]. Third, the sign of the slope of (H^*, T^*) band in systems having FM ground state [see Fig. 1(a)] is different than the systems having AFM as the ground state [see Fig. 1(b)]. The slope of these bands are dictated by the fact that the FM phase exists over a larger temperature range at higher fields. The same argument can be followed for (H^{**}, T^{**}) band also, which will be shown later on. The slope of (H_K, T_K) band can be understood from similar arguments that if AFM (FM) is the high-T phase, kinetic arrest of the high-T phase during cooling must be observed at low (high) fields [13,32]. In Fig. 1(a), when the sample is cooled along AB, note that for both regions 1 (R1) and 2 (R2), $T_K > T^*$, and therefore, these regions will be arrested and persist in the high-T AFM phase as T^* is ineffective along AB. Along Path EF, for both R1 and R2, $T^* > T_K$. Hence, both regions will transform into FM phase and T_K laying below T^* is ineffective as the transformation to low-T equilibrium phase has already happened. However, along CD, note that $T_K(R1) > T^*(R1)$ but $T_K(R2) < T^*(R2)$. Therefore R1 will remain in AFM phase, whereas R2 will transform into FM. Therefore path CD will give rise to phase coexistence of equilibrium FM phase and glasslike arrested AFM phase. It essentially appears due to overlapping of disorder broadened (H_K, T_K) and (H^*, T^*) bands. In conclusion, different cooling paths produce different states at low temperature. Similarly, in Fig. 1(b), cooling along AB and EF result into complete transformation and arrest of the two regions, respectively. While cooling through band overlapping region (along CD) will give rise to phase coexistence.

Here, we will investigate the nonequilibrium behavior of the kinetically arrested glasslike state at low temperature [14]. Now, consider the schematic in Fig. 1(a) which explains the systems having FM as low-T equilibrium phase. Let the sample is cooled at $H = 0$ (along AB), then both R1 and R2 will remain arrested. Now, if H is raised to H_1 and the arrested system is warmed along path GJ, we can obtain two interesting conditions as a function of temperature. First, consider the temperature at $T = T_2$. Note that, for the region R2, $T_2 = T_K$, therefore R2 will devitrify into FM phase. While R1 will remain arrested, because for R1, T_K lies at higher temperature than the probing temperature T_2. Also note that, at T_2, $T_2 < T^*$ for the region R2. Therefore there is no free energy barrier [see Fig. 1(c)] and the kinetically arrested region R2 will spontaneously devitrify into the equilibrium phase. The rate of devitrification (or relaxation rate) will increase with increase in the temperature due to increased thermal energy. Now consider, at higher temperature $T = T_1$. Here, $T_1 = T_K > T^*$ for the region R1, i.e., in region R1, the arrested high-T phase will transforms into equilibrium phase. However, in this case, there exist a finite energy barrier [see Fig. 1(d)] where the high-T state is trapped. So, it needs to overcome the barrier to transform to the equilibrium phase. Now, as temperature increases, simultaneously, the energy barrier also increases. As a result, the transformation rate will decrease with the rise in temperature. Therefore, while warming from a glasslike arrested state, there will be crossover from $T_K < T^*$ to $T_K > T^*$. In the temperature range, $T_K \leqslant T < T^*$ [see Fig. 1(c)] there is no free energy barrier, but $T \geqslant T_K > T^*$ [see Fig. 1(d)], there is a finite barrier. Now instead of H_1, if the arrested state is warmed at higher fields, say $H = H_2$ (along KL), then the crossover will occur at lower temperature as evident from the Fig. 1(a) because T_Ks of R1 and R2 lie at lower temperatures (marked as stars) at higher fields.

II. EXPERIMENTAL DETAILS

Polycrystalline samples of PCMAO and LCMO have been prepared by conventional solid state and pyrophoric methods, respectively [14,33]. Magnetic measurements are performed in 16 T vibrating sample magnetometer (M/S Quantum design, USA). T dependence of magnetization (M) have been measured in zero field cooled (ZFC), field cooled cooling (FCC) and field cooled warming (FCW) modes. In ZFC, the sample is initially cooled in absence of external field and the M-T data are recorded while warming in presence of certain H. In FCC, M is recorded while cooling the sample in presence of a fixed H. In FCW, M is recorded while warming the sample after it is cooled at the same H. The temperature sweep rate during M-T measurements is 1 K/min. Field cycles have been performed at 80 Oe/sec rate. While the samples are initially cooled at $H = 0$, the cooling rate is 10 K/min (in Fig. 3

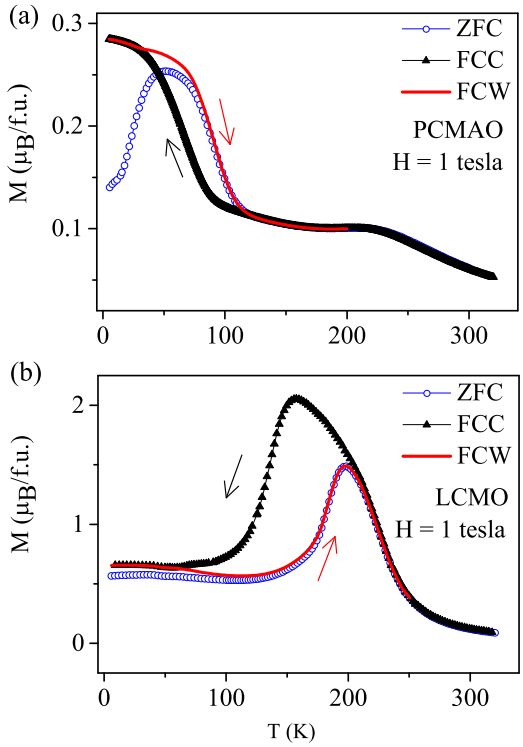

FIG. 2. Temperature (T) variation of magnetization M of (a) PCMAO and (b) LCMO at $H = 1$ T measured in ZFC, FCC and FCW modes. The arrows indicate the direction of temperature sweep during measurements. Thermal hysteresis between FCC and FCW curves is due to the first-order transition between AFM and FM phases.

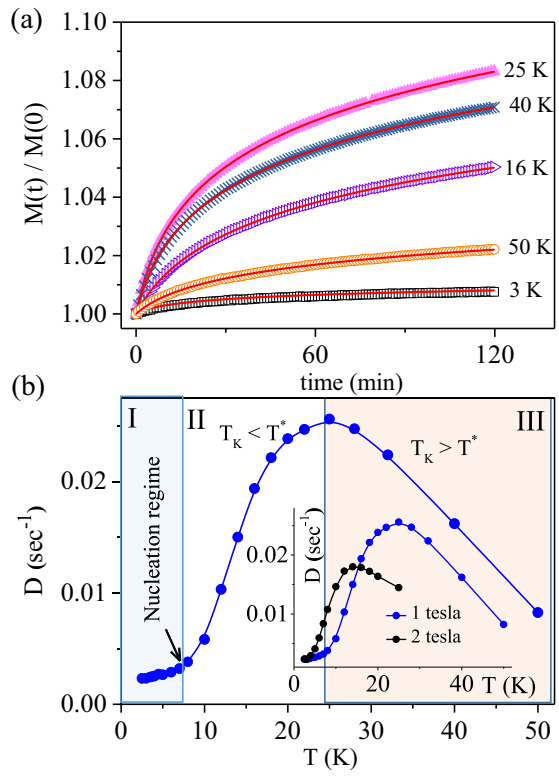

FIG. 3. (a) Time dependence of magnetization at different measurement temperatures in PCMAO. The sample is initially cooled at $H = 0$ down to $T = 2$ K and then raised to the measurement temperatures after applying a magnetic field of $H = 1$ tesla. See text for more details. Solid lines are fitted curves by using Eq. (2). (b) Variation of "D" as obtained from fitting the relaxation data by using Eq. (2). In the inset, we have shown the variation of "D" for two measurement fields, $H = 1$ and 2 T by following the same cooling and measurement protocols.

and Fig. 2). In the phase-coexisting state at low temperature, the volume fractions of the two phases have been calculated from the M value at required temperature, suppose, $M(T_m)$ at temperature T_m, using the method described in Ref. [34]. If the FM volume fraction is $f_{\rm FM}$ [so AFM volume fraction is $(1 - f_{\rm FM})$] at T_m, the $f_{\rm FM}$ is given by the relation

$$M(T_m) = f_{\rm FM}(M_0 + \alpha \times H_m) + (1 - f_{\rm FM}) \times \beta \times H_m \quad (1)$$

Here, α and β are the susceptibilities of the FM and AFM phases, respectively, which are obtained from the slope of the M-H curve at temperature T_m. M_0 is the spontaneous magnetization of the FM phase and H_m is the measurement field. In this context, we would like to mention here that x-ray diffraction studies are also useful tool for this purpose [35,36], however, only in those systems where the high and low-T phases have different structural parameters. Neutron scattering measurement has been also employed [37]. However, the resolution of these scattering based techniques are much limited than the magnetization measurements, which has very high relative accuracy. This is due to the fact that slight change in relative volume fraction of the FM and AFM phases will give rise to a large change in magnetization.

III. EXPERIMENTAL RESULTS

PCMAO and LCMO are paramagnets (PM) at room temperature. As T is reduced, PCMAO undergoes the PM → AFM → FM transitions. The AFM to FM transition is first order. On the other hand, LCMO shows PM → FM → AFM phase transitions with the reduction in T and the FM to AFM transition is first order in nature. PCMAO and LCMO have opposite high and low-T phases. In case of PCMAO, the AFM to FM transition is completely arrested below (H_K, T_K) if the sample is cooled at $H = 0$ [see Fig. 1(a), path AB]. Therefore, because of the kinetic arrest, the zero field cooled state of PCMAO remains entirely in the AFM phase and transform to the FM phase while heating. However, when it is cooled in presence of finite H [$0 < H < 10$ T, along CD in Fig. 1(a)], the AFM to FM transition is partially arrested due to overlapping of the (H^*, T^*) and (H_K, T_K) bands. As a result, phase coexistence persists till the lowest temperature. At $H \geqslant 10$ T [along EF in Fig. 1(a)], the AFM to FM transition occurs fully and the magnetic state below (H^*, T^*) is homogeneous FM [15]. On the contrary, in case of LCMO, when it is cooled at very high fields [$H > 8$ T, see path EF in Fig. 1(b)], the FM to AFM transition is completely arrested and the sample remains entirely in the FM phase down to lowest temperature. The high- and low-T phases coexist when LCMO is cooled at intermediate fields [$0 < H < 8$ T, see path CD in Fig. 1(a)]. In Figs. 2(a) and 2(b), we have shown the

M-T data of PCMAO and LCMO respectively at $H = 1$ T in ZFC, FCC, and FCW modes. Evidently, in the field cooled state of both the systems, the low-T state is a mixture of FM and AFM phases which persists even below the closer of thermal hysteresis. However, it must be kept in mind that in phase coexisting state of PCMAO and LCMO, the AFM and FM respectively are the nonequilibrium phases because these are actually the high-T phases but persist at low temperature due to incomplete phase transition. The volume fraction of the equilibrium and nonequilibrium phases change with time (glassy behavior) and when the applied field is changed.

In Fig. 3, we have shown the effect of temperature on the dynamics of the devitrification process of the kinetically arrested AFM state in PCMAO while warming by measuring the time (t) dependence of M at different temperatures. To perform these measurements, we have first cooled the sample down to lowest temperature, $T = 2$ K at external field $H = 0$, so that the transition from high-T AFM to low-T FM state is entirely arrested and hence AFM state remains down to $T = 2$ K [see path AB in Fig. 1(a)]. Then a finite field $H = 1$ T is applied at $T = 2$ K and holding the same field, the temperature is raised [see path GJ in Fig. 1(a)] to the probing temperature, say $T_p = 3$ K at 0.5 K/min heating rate. After temperature becomes stable, change in M with "t" is measured for next 2 hours. After the M-t measurement, the sample is warmed to the room temperature (paramagnetic state). The same protocol is repeated for different values of T_ps. In Fig. 3(a), we have shown M-t data at few selected temperatures for clarity. We would like to mention here that, the reason behind following such protocol is, when PCMAO is warmed at finite H after cooling at $H = 0$, the kinetically arrested AFM state will devitrify into the equilibrium FM state and we can study its dynamics at various temperatures. There are a few interesting features which are clearly visible in Fig. 3(a). First, M increases with t at every temperature which is essentially due to transformation of the kinetically arrested AFM phase into the equilibrium phase which is the FM state at low temperatures. Second, initially relaxation rate increases with the rise in T till $T_p = 25$ K, then starts reducing on further rise in T. This nonmonotonic behavior can be reconciled by the crossover from $T_K < T^*$ to $T_K > T^*$ condition described earlier [see Figs. 1(a), 1(c), and 1(d)].

To gain further insight of the data, we have fitted M-t curves by following the equation

$$M(t) = M(0)[1 + D\ln(t/\tau)]. \quad (2)$$

Here D is the rate constant and $M(0)$ is the initial value of magnetization (at $t = 0$) [18]. We have plotted the variation of D against T in Fig. 3(b). Note that, we can divide the entire temperature regime into three segments. In segment I, D increases very slowly with T, in segment II, D rises rapidly with T till $T_p = 25$ K and in segment III, D decreases with further increase in T. Combination of segments I and II, the curve mimicks an overall "S" shape curve, which is similar to relaxation kinetics observed across a first-order phase transition where the dynamics is controlled by nucleation and growth mechanism [38]. In addition, at higher fields [see the inset of the Fig. 3(b)] the curve is shifted towards lower temperature which can be understood from the schematic in Fig. 1(a). See the paths GJ and KL in Fig. 1(a) at fields H_1 and H_2, respectively.

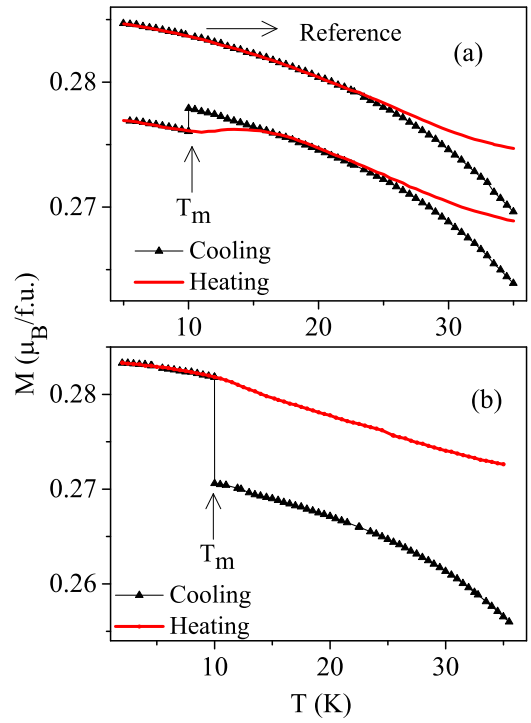

FIG. 4. Memorylike effect in PCMAO which are measured by following (a) protocol 1 and (b) protocol 2. Here, $H_m = 1$ T and $T_m = 10$ K. The reference curve in (a) shows that the usual FCC and FCW curves are completely merged below $T = 25$ K. However, if protocols 1 and 2 are followed, the M-T curves show memorylike responses at the probing temperature $T_m = 10$ K. Details of protocols 1 and 2 are described in the text.

Now, by following two different measurement protocols, we shall demonstrate another manifestation of the acute nonergodicity of the magnetic glass state which appears like the memory effect [7]. Protocol 1 is one of the conventional ways to check the memory effect in glasses. For PCMAO, in protocol 1, initially a measuring field, $H_m = 1$ T is applied at $T = 320$ K and the sample is cooled at 1 K/min rate from $T = 320$ to 5 K and subsequently heated back to record a reference curve. These are the usual FCC and FCW measurements. Then at same H_m and cooling rate, the sample is again cooled down to a probing temperature, say $T_m = 10$ K, which lies below the closure of thermal hysteresis. At T_m, H is reduced to zero. After a waiting period of $t_w = 3$ hours, H is increased back to H_m and cooling is resumed down to T = 5 K. The sample is subsequently warmed without changing the field. M is recorded in every cooling and heating cycles. The results are presented in Fig. 4(a), where we have shown both the reference curve and the M-T curve undergoing the field cycling. One should note here that T_m is chosen below the closer of the hysteresis because across the hysteresis, the dynamics of the first-order transition will also play a role and we can not purely characterize the MG state. In protocol 2, the sample is cooled in presence of $H_m = 1$ T from $T = 320$ K to $T_m = 10$ K as in protocol 1 and at T_m, H is increased from 1 to 2.5 T instead of reducing it to zero and kept there for $t_w = 60$ sec. After the

waiting period of t_w, H reduced to $H = 1$ T. Then the cooling and subsequent heating is followed like in protocol 1 and M has been measured during every cooling and heating cycles. The data are shown in Fig. 4(b). It may be noted here that the protocol 2, where H is increased, is not a conventional way to check for memory effect. In protocol 1, when PCMAO is cooled at $H_m = 1$ T down to $T_m = 10$ K, it consists of 4.1% volume fraction of FM and rest AFM state due to kinetic arrest of the first-order AFM to FM transition. Then the reduction in H and a temporary stop for t_w at $H = 0$ cause a small fraction of the FM phase to convert into the AFM phase, so that after the aging time of t_w, when $H = 1$ T is reapplied, M has a downward discontinuous jump at $T_m = 10$ K in cooling path due to reduced amount of the FM phase fraction. From the value of M, the estimated volume fraction of the FM phase after field cycle is 4.0%. As the sample is subsequently cooled down to $T = 5$ K and reheated, M shows an upward jump above $T_m = 10$ K and merges back to the cooling curve [see Fig. 4(a)]. This indicates that during heating, the system recovers the 0.1% of FM phase fraction that transformed into AFM phase due to field cycle and the waiting time t_w while cooling the sample. Similarly, in protocol 2, during cooling when a field cycle is performed from $1 \rightarrow 2.5 \rightarrow 1$ T at T_m, it causes field induced conversion of AFM phase into FM phase. As a result, M shows an upward discontinuous jump at T_m in cooling path due to increased FM phase fraction after the field cycle. In this case, M values before and after the field cycle indicate that the FM volume fraction increased from 3.8% to 4.2% due to H cycle at $T_m = 10$ K. In the heating path, M shows a slight but noticeable discontinuity above T_m [see Fig. 4(b)] due to conversion of the FM to AFM phase. However, unlike in protocol 1, here heating curve does not merge with the cooling curve. This implies that the system failed to completely recover the FM and AFM phase fraction.

In case of LCMO, the first-order transition occurs from FM at high temperature to AFM phase at low temperature. Therefore the phase coexisting state at low temperature contains mixture of FM and AFM phases but the AFM is the equilibrium phase, which is opposite to the case of PCMAO. In this case, we have followed similar protocols except that, while following protocol 1, LCMO is cooled at $H_m = 9$ T and it is reduced to zero at $T_m = 15$ K for $t_w = 6$ hours. In protocol 2, the sample is cooled at $H_m = 3$ T down to $T_m = 15$ K, and H is raised from 3 to 10.5 T and kept there for $t_w = 60$ sec and again reduced to 3 T. The results for LCMO are shown in Figs. 5(a) and 5(b), respectively. Following protocol 1, when we cool LCMO in presence of $H_m = 9$ T, it completely arrest the FM to AFM transition. So reference curve does not show the FM to AFM transformation in cooling path unlike observed in Fig. 2(b). As a result, the low temperature phase contains the FM phase, which is actually the nonequilibrium phase. The cooling curve with a temporary stop at $T_m = 15$ K shows step similar to PCMAO, which corresponds to decrease in FM volume fraction by 4.5%. Subsequent warming curve shows a large discontinuity above $T = 15$ K. However, the heating curve does not immediately merge with the cooling curve, i.e., the system is unable to recover the entire volume fraction just above T_m. Nonetheless, it merges with the cooling curve at a much higher temperature [see the main panel of Fig. 5(a)], which will be explained in the discussion section.

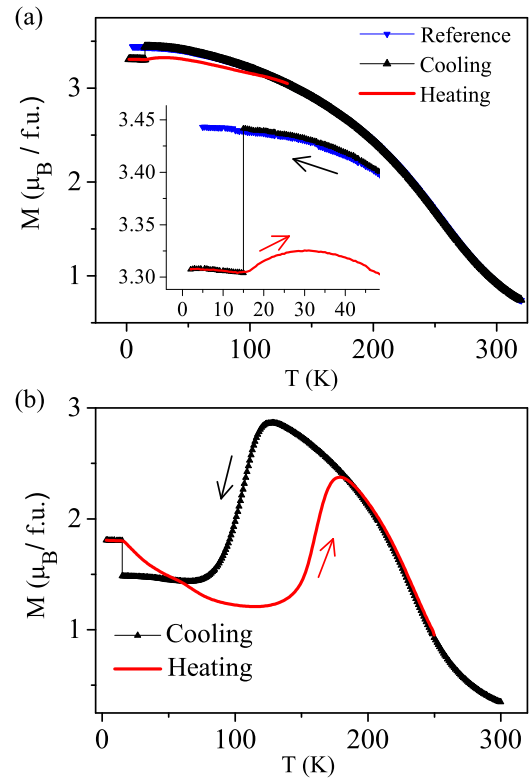

FIG. 5. Memorylike effect in LCMO. (a) H is reduced to zero at 15 K (protocol 1). Reference curve is the usual FCC curve and does not show the FM to AFM transition due to kinetic arrest (b) H is increased to 10.5 T at 15 K (protocol 2).

In protocol 2, during cooling M shows discontinuity due to the field cycle, which corresponds to an increase in FM volume fraction from 44.0% to 54.4%. The M-T curve in the subsequent heating cycle merges with the cooling curve which means that the system completely recovers the volume fraction of the coexisting FM and AFM phases of the field cooled state. Therefore, in the case of LCMO, in the cooling path the decrease or increase in H results into decrease or increase in FM volume fraction at $T_m = 15$ K, which the system tries to recover while heating. It should be mentioned here that in case of LCMO also, the T_m is chosen keeping in mind that it is below the closure of thermal hysteresis, so that kinetics of the first-order transition does not intervene. We have performed many similar measurements using different values of H_m, T_m, and t_w for both samples. All these parameters affect the recovery of phase fraction during heating depending on the amount of phase conversion between FM and AFM in the cooling cycle due to field cycle.

To further elucidate the observations, we have performed thermal cycle measurements which are shown in Figs. 6(a) and 6(b) for PCMAO and LCMO, respectively. For both samples, we have basically followed protocol 1 with some modifications in the final heating cycle. In case of PCMAO [see Fig. 6(a)], we have initially cooled the sample at $H = 1$ T to $T_m = 10$ K and reduced H to zero. After the waiting time of $t_w = 3$ hours, we have reapplied $H = 1$ T and cooled the sample to $T = 5$ K. The sample is then subsequently warmed holding the same field. However, instead of continuous heat-

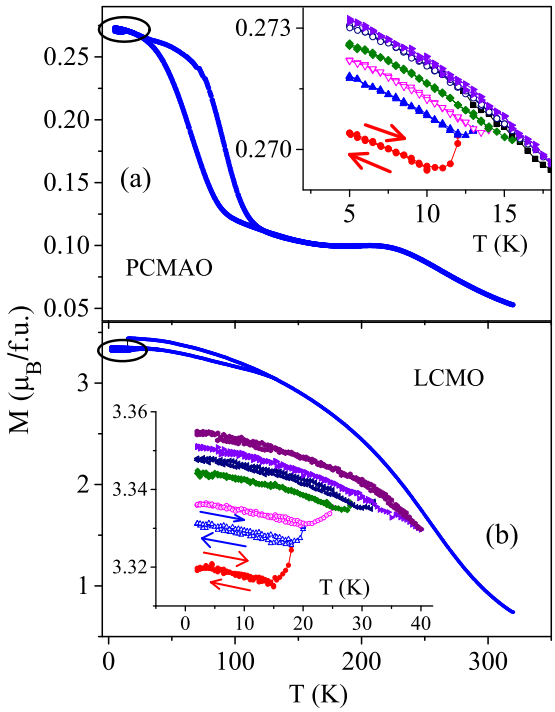

FIG. 6. Effect of thermal cycle performed on (a) PCMAO in presence of $H = 1$ T and (b) LCMO in presence of $H = 9$ T. In both cases, M increases after each thermal cycle performed from progressively higher T, which indicates that the AFM phase transforms into FM phase during warming.

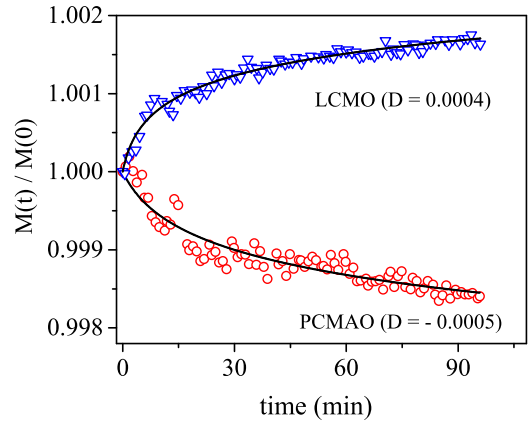

FIG. 7. Variation of $M(t)/M(0)$ with time at $T = 10.5$ and 18 K for PCMAO and LCMO, respectively, where $M(0)$ and $M(t)$ are the M at time $t = 0$ and t. In case of LCMO, the measurement is performed similar to protocol 1. Whereas, in case of PCMAO, the measurement is performed similar to protocol 2. Solid black lines are the fitted curves by using Eq. (2). Values of rate constant, D are also mentioned in the figure.

ing through T_m, we have performed multiple thermal cycles. The cycles are performed as follows: $T = 5 \rightarrow 12 \rightarrow 5$ K, then $5 \rightarrow 13 \rightarrow 5$ K, $5 \rightarrow 14 \rightarrow 5$ K, $5 \rightarrow 16 \rightarrow 5$ K and $5 \rightarrow 20 \rightarrow 5$ K with simultaneously recording M-T response. In the inset of Fig. 6(a), we have shown the magnified view of the thermal cycles and represented different cycles in different colors. We see that after each cycle, M at $T = 5$ K increases which suggests that AFM phase is transforming into the FM state during heating. Similar measurement in case of LCMO performed at $H_m = 9$ T is shown in Fig. 6(b). Here, we have cooled the sample at $H_m = 9$ T to $T_m = 15$ K and reduced the field to zero for a waiting time of $t_w = 6$ hours. After 9 T field is reapplied, we have cooled the sample to $T = 5$ K. In the following warming path at same H, we have performed thermal cycles as follows: $T = 5 \rightarrow 15 \rightarrow 5$ K, then $5 \rightarrow 20 \rightarrow 5$ K, $5 \rightarrow 25 \rightarrow 5$ K, $5 \rightarrow 28 \rightarrow 5$ K and $5 \rightarrow 32 \rightarrow 5$ K, and $5 \rightarrow 40 \rightarrow 5$ K with simultaneously recording the M-T response. The magnified data of the thermal cycles is shown in the inset of Fig. 6(b). It gives identical result that M at $T = 5$ K increases after each cycle which implies the conversion of the AFM phase into FM. Therefore it further confirms that during heating, the AFM phase transform into FM phase which was converted into AFM state during cooling by reducing the field to zero and waiting for the time period of t_w. It gives further evidence that in these systems, when the phase fraction is disturbed by H cycle at a temperature T_m in the cooling process, the phase fraction is fully or partially recovered by reverse transformation above T_m.

To further bring out the nonequilibrium behavior of these two systems, we have carried out a few time (t) dependent M measurements and have shown the data in Fig. 7. In case of LCMO, initially the sample is cooled at 1 K/min cooling rate in presence of $H = 9$ T down to $T = 15$ K and H is reduced to zero. After a waiting time of $t_w = 6$ hours, $H = 9$ T is reapplied and the sample is cooled to $T = 5$ K and subsequently warmed to $T = 18$ K without changing the field. After stabilizing the temperature at 18 K, isothermal change in M with time is measured for nearly, $t = 1.5$ hours holding the same field. M is found to monotonically increase with time. This indicates towards the gradual transformation of the AFM to FM phase with time. On the other hand, in case of PCMAO, it is cooled in presence of $H = 1$ T down to $T_m = 10$ K and increased H to 3 T. After a waiting time of $t_w = 60$ sec, H is reduced back to 1 T and the sample is cooled down to $T = 5$ K. Without changing H, the sample is rewarmed to $T = 10.5$ K and isothermal variation of M with time is measured for nearly 1.5 hours. M reduces with time which indicates the gradual transformation of FM to the AFM phase. One may note that the protocols used for LCMO and PCMAO in these measurements are basically similar to the earlier protocols 1 and 2, respectively [see Figs. 5(a) and 4(b)]. These relaxation measurements further reveal the nonequilibrium nature of the magnetic state.

IV. DISCUSSION

In Fig. 8, we have shown the schematic H-T phase diagram of a kinetically arrested first-order transition, where the transition occurs from the high-T AFM to low-T FM phase [13]. This is essentially same as Fig. 1(a), but now it includes (H^{**}, T^{**}) band also and has been drawn for four different regions in the sample (1–4). Therefore this schematic explains the magnetic response of PCMAO. We will denote the regions 1, 2, 3, and 4 as R1, R2, R3, and R4 hereafter. We have also marked different positions in the H-T plane as star and

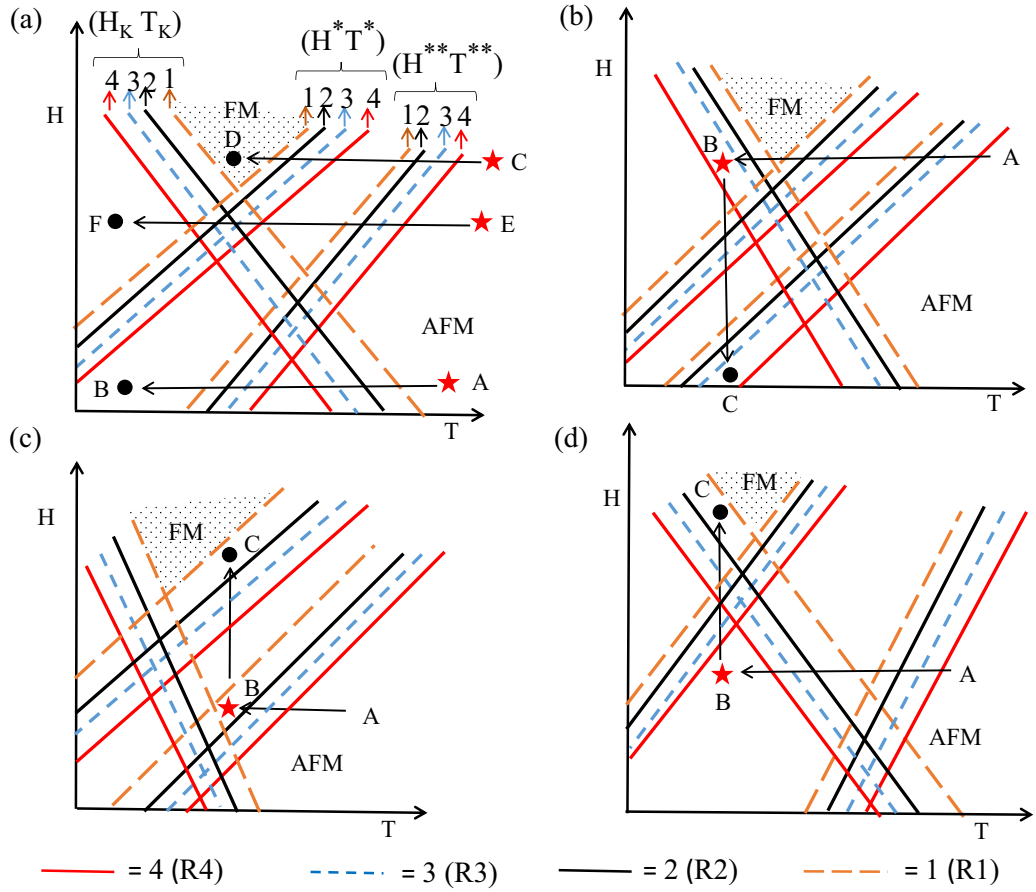

FIG. 8. H-T phase diagram of kinetically arrested first-order transition for PCMAO. The lines correspond to the (H^*, T^*), (H^{**}, T^{**}), and (H_K, T_K) of different regions of the sample as mentioned at the bottom of the figure. (a) shows that different cooling paths produce different magnetic states at low temperature. Along AB, all regions are arrested at high-T AFM state, along CD, the first-order transition from AFM to FM in all four regions. EF produces phase coexistence. (b) to (d) demonstrate the possible scenarios which explain the memorylike magnetic responses shown in Fig. 4. See the text for details.

filled circle to explain the effect of different paths traversed in the H-T plane during measurements by following protocols 1 and 2.

If PCMAO is cooled along AB [see Fig. 8(a)], all four regions (R1, R2, R3, R4) of the sample encounter the (H_K, T_K) band before their (H^*, T^*) and hence get kinetically arrested in the high-T AFM phase. As a result, the high-T AFM in all four regions of the sample do not undergo any transition and remain in the AFM phase till the lowest temperature. On the other hand, if the sample is cooled at very high fields, say along CD, all four regions encounter the (H^*, T^*) band before their respective (H_K, T_K) and undergo the usual first-order transition to low-T equilibrium FM phase. Cooling at intermediate fields, for instance, along EF, due to overlapping of the (H^*, T^*) and (H_K, T_K) bands, it gives rise to phase coexistence, i.e., some regions (in this case R4 and R3) encounter (H^*, T^*) first, and transform into FM, whereas some regions (R2 and R1) get kinetically arrested in the AFM phase due to higher (H_K, T_K). Therefore the volume fraction of the two phases can be tuned by varying the cooling field. The magnetic response which is shown in Fig. 4(a) can be understood from the schematic in Fig. 8(b). Suppose, we have cooled PCMAO along AB, so that when we have reached point B (red star), all four regions R1, R2, R3, and R4 have approached the (H^*, T^*) band before (H_K, T_K) and have transformed into the low-T FM phase. Now, if H is reduced to zero along BC and reach point C (black filled circle), R1, R2, and R3 encounter their superheating temperatures (H^{**}, T^{**}). As a result, these regions transform into the high-T phase i.e., the AFM phase. This occurs because above (H^{**}, T^{**}), the high-T phase is the equilibrium phase. As H is increased again along path CB and reach point B again, these regions remain in the AFM phase. However, when we reheat the sample, these regions encounter the (H_K, T_K) band and undergo dearrest. As a result, they transform into the FM phase during heating. It means that R1, R2, and R3 have transformed into AFM when H is reduced to point C but during reheating all of them have converted back to the FM phase. Hence it recovers the entire volume fraction as observed in Fig. 4(a).

On the other hand, the memorylike response, which is shown in Fig. 4(b), has two distinct features. First, during heating FM transforms into AFM phase and second, the recovery of the volume fraction is not complete. These features can be understood from the schematics 8(c) and 8(d). It involves two distinct processes that occur simultaneously when H is increased and subsequently reduced during cooling at $T_m = 10$ K (protocol 2). Both processes occur simultaneously but at different regions of the sample because of the

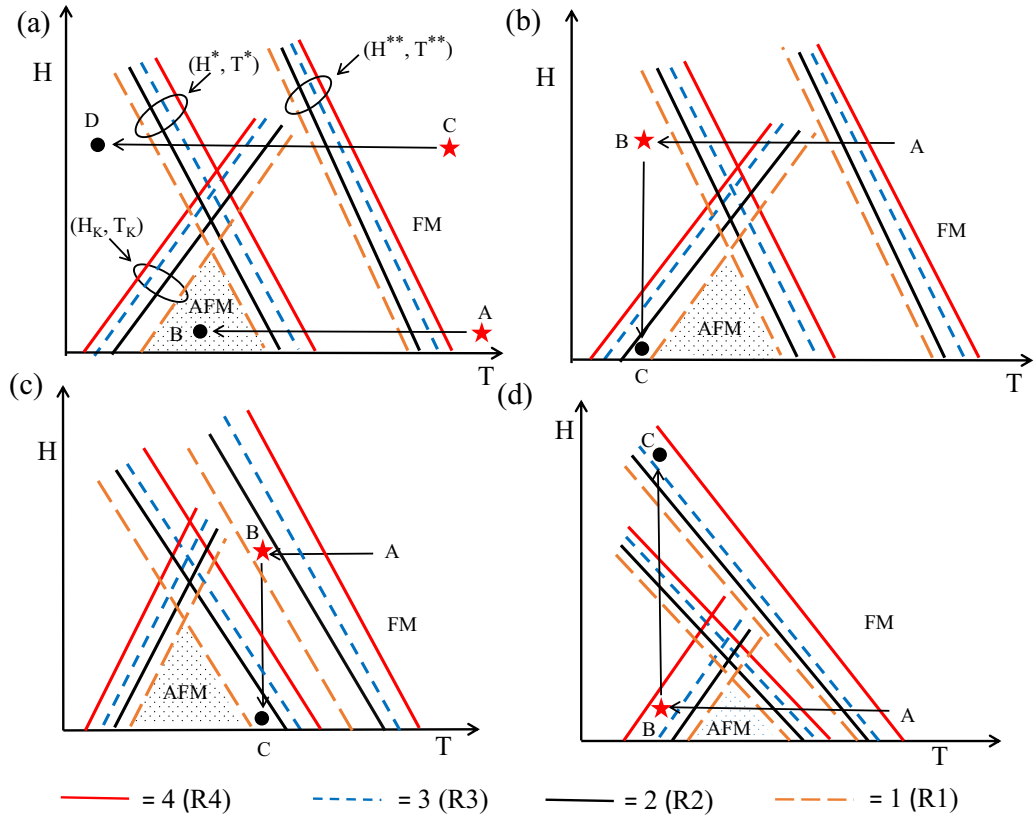

FIG. 9. H-T phase diagram of kinetically arrested first-order transition for LCMO. The lines correspond to the (H^*, T^*), (H^{**}, T^{**}), and (H_K, T_K) of different regions of the sample as mentioned at the bottom of the figure. (a) shows different cooling paths produce different magnetic states at low temperature. Along AB, all regions transform to AFM phase, so that low temperature state is a homogeneous AFM phase. Along CD, All regions are arrested in FM phase, so that low temperature magnetic state is kinetically arrested FM phase. (b) to (d) demonstrate the possible scenarios which can explain the memorylike magnetic responses shown in Fig. 5. See the text for details.

spatial distribution of the transition temperatures in the sample in a wide H-T region. One of the processes is shown in Fig. 8(c). When the sample is cooled along AB, R4, R3, and R2 remain in the AFM phase, because at point B, these regions are much above (H^*, T^*) band. Note that, regions are close to their (H^{**}, T^{**}). When H is increased along BC, these regions approach the (H^*, T^*) band and transform into the FM phase at point C. When we subsequently reduce H and heat the sample along the reverse paths CB and BA, respectively, these regions immediately transform into AFM phase when they approach (H^{**}, T^{**}) band. Another scenario is possible in this protocol which we have shown in Fig. 8(d). Cooling along AB will arrest the high-T AFM phase. When we increase H, R4, R3, and R2 encounter the (H_K, T_K) band and devitrify into FM. In the reverse H decreasing cycle, these FM regions remain in the FM phase. When we subsequently heat the sample along BA, the FM transforms into AFM near (H^{**}, T^{**}) band which lies at very high temperature. Therefore, in the first process, the FM phase immediately undergo reverse transformation to AFM phase during heating, while in the second process, the FM phase does not immediately transform back to the AFM phase. Therefore these two independent processes which occur together, can explain the magnetic response shown in Fig. 4(b). It means that one process occurs in some part of the sample, whereas the other process occurs at some other regions, where the above described conditions are satisfied. The relative contribution of these two processes at any H_m and T_m will decide the volume fraction in the entire systems which it can regain during heating. Hence, it will decide the memorylike response in protocol 2 in PCMAO. It may be noted here that the band diagrams of (H^*, T^*), (H^{**}, T^{**}), and (H_K, T_K) in all the figures, i.e., Figs. 8(a)–8(d), are not exactly identical, for example, the slope of the bands, the distance between the lines representing the regions R1 to R4, etc. This has been done intentionally because it indicates that although the measurements have been performed at a particular temperature (i.e., $T_m = 10$ K) and within particular range of H, as these bands are distributed in a large H-T landscape throughout the real space of the sample, the above described scenarios may be satisfied in different regions of the sample. Ultimately we are measuring the bulk response and hence all these processes will contribute.

The memorylike effect in LCMO which are shown in Fig. 5 can be similarly understood from the interplay of (H^*, T^*), (H^{**}, T^{**}), and (H_K, T_K) bands. We have shown the schematic in Fig. 9. It is phenomenologically identical to Fig. 1(b), but now includes all the three bands and represents four regions (R1, R2, R3, and R4) in the sample. Figure 9(a) shows the framework of the kinetic arrest in LCMO. When the sample is cooled along path AB, all the regions (R1, R2, R3, and R4) encounter the (H^*, T^*) band before (H_K, T_K) and undergo the first-order transition from the high-T FM to low-T AFM

phase. On the other hand, if the sample is cooled at high fields, such as along CD, all four regions are arrested in the high-T FM phase and the transition is not observed. Note that, due to opposite low and high-T states in LCMO, kinetic arrest also results into opposite situation compared to PCMAO.

The memorylike phenomenon of LCMO shown in Fig. 5(a) has two distinct features. First, while showing memory above T_m during final heating, AFM phase transform into FM, that is evident from the fact that M increases with rise in T. Second, the transformation is not complete. Therefore the situation is somewhat similar to Fig. 4(b) in the context that the phase fraction is recovered partially during heating. Therefore, in case of LCMO also, the response can be understood by combining two independent processes. We have described these two different processes in the schematic of Figs. 9(b) and 9(c). Consider Fig. 9(b), when the sample is cooled along AB down to point B, all the four regions (R1–R4) remain kinetically arrested in FM phase. When H reduced to zero to point C, R4, R3, and R2 cross their (H_K, T_K) and get dearrested into the equilibrium phase, i.e., transform into AFM phase. Subsequently, when H is increased to its previous value to point B, these AFM phase will remain in the AFM phase. After that, when the sample is heated along path BA, these regions will transform into FM phase near the (H^{**}, T^{**}) band which lies at much higher temperature. Therefore these regions will not immediately transform just above the probing temperature T_m. Apart from this, another situation may simultaneously occur in some different region of the sample, which is shown in Fig. 9(c). In this case, when LCMO is cooled along AB down to point B, all the regions will remain in the FM phase, because both (H^*, T^*) and (H_K, T_K) bands lie at much lower temperatures. However, when H is reduced to zero, R2, R3, and R4 cross the (H^*, T^*) band and transform into AFM phase. Subsequently, when H is increased back to point B and followed by reheating along BA, the AFM phase will immediately transform into FM phase due to the presence of (H^{**}, T^{**}) band, which is active during heating. Therefore, in the first mechanism [see Fig. 9(b)], some FM volume fraction transform into AFM phase along BC but does not immediately transforms into FM phase in the final heating along BA. However, in the second process [see Fig. 9(c)], the FM volume fraction which transform into AFM phase during reduction of H (along BC), transform back to FM phase immediately during warming (along BA). Thus these two separate processes together explain the magnetic response in Fig. 5(a), where the system partially regain the phase fraction during heating.

On the other hand, the memorylike effect shown in Fig. 5(b) can be understood from the schematic which we have shown in Fig. 9(d). Suppose, the sample has been cooled along AB. During cooling all four regions (R1–R4) will transform from the high-T FM phase to the low-T AFM phase because they cross the (H^*, T^*) band before (H_K, T_K). When H is increased along path-BC up to point C, R1, R2, and R3 will transform into FM phase because they encounter (H^{**}, T^{**}) at high H. When H is subsequently reduced to point B along path CB, these regions will remain in the kinetically arrested FM phase. During next heating, these regions will immediately transform back into the equilibrium AFM phase while crossing the (H_K, T_K) band. This dearrest will cause M to reduce during heating above T_m.

Therefore the interplay of these bands related to the first-order phase transition can give rise to the memorylike effect. However, it should be mentioned that there is a difference between the signature of spin glass and magnetic glass. In spin glasses, while showing the memory effect during heating, it returns to the old state in both field increasing and decreasing cycles [7]. On the contrary, in MGs, the memorylike effect depends also on the nature of its equilibrium phase. Therefore, using both of the measurement protocols, i.e., increasing as well as decreasing H at the measurement temperature (T_m), a spin-glass-like state and MG glass can be distinguished. In addition, the ground state of the MG glass can also be identified. It should be noted further, that in last two decades, there are several experimental studies that report the memorylike phenomena in phase separated systems [39–43]. Such behaviors are also likely to be explained in the framework of the above described model.

V. SUMMARY

In a nutshell, we present a few nonequilibrium magnetic response in the magnetic glass state of PCMAO and LCMO. We have first shown the evolution of the dynamics of a kinetically arrested phase with increasing temperature and also studied the effect of magnetic field. In addition, we have experimentally shown that if the phase fraction is tampered during cooling by changing H, the system regain the fraction during heating. These appear similar to the memory effect observed in other glassy systems, like spin glass, etc. Finally, we demonstrate that such magnetic behavior can be explained in the framework of kinetic arrest of the associated first-order phase transition. Essentially, the interplay of supercooling, superheating and kinetic arrest of a disorder broadened transition in the H-T plane gives rise to such nonequilibrium response of the phase coexisting states. In addition, identification of the ground state is a fundamental aspect of a phase coexisting state and tricky as well. In that case, combined use of the two protocols described here can easily distinguish the ground state of the system.

ACKNOWLEDGMENT

We acknowledge Dr. S. B. Roy for relevant discussions regarding this work.

[1] K. Jonason, E. Vincent, J. Hammann, J. P. Bouchaud, and P. Nordblad, Phys. Rev. Lett. **81**, 3243 (1998).

[2] N. C. Keim, J. D. Paulsen, Z. Zeravcic, S. Sastry, and S. R. Nagel, Rev. Mod Phys. **91**, 035002 (2019).

[3] C. Scalliet and L. Berthier, Phys. Rev. Lett. **122**, 255502 (2019).

[4] I. L. Morgan, R. Avinery, G. Rahamim, R. Beck, and O. A. Saleh, Phys. Rev. Lett. **125**, 058001 (2020).

[5] V. Dupis, F. Bert, J.-P. Bouchand, J. Hammann, F. Ladieu, D. Parker, and E. Vincent, Pramana J. Phys. **64**, 1109 (2005).

[6] A. Samarakoona, T. J. Satob, T. Chena, G.-W. Cherna, J. Yanga, I. Klicha, R. Sinclairc, H. Zhouc, and S.-H. Lee, Proc. Natl. Acad. Sci. U.S.A. **113**, 11806 (2016)

[7] S. Pal, K. Kumar, A. Banerjee, S. B. Roy, and A. K. Nigam, Phys. Rev. B **101**, 180402(R) (2020).

[8] F. Rivadulla, M. A. Lopez-Quintela, and J. Rivas, Phys. Rev. Lett. **93**, 167206 (2004).

[9] Y.-k. Tang, Y. Sun, and Z.-h. Cheng, Phys. Rev. B **73**, 012409 (2006).

[10] S. Wang, J. Zhang, G. Cao, C. Jing, and S. Cao, Phys. Rev. B **76**, 054415 (2007).

[11] A. Bhattacharyya, S. Giri, and S. Majumdar, Phys. Rev. B **83**, 134427 (2011).

[12] M. K. Chattopadhyay, S. B. Roy, and P. Chaddah, Phys. Rev. B **72**, 180401(R) (2005).

[13] A. Banerjee, K. Mukherjee, K. Kumar, and P. Chaddah, Phys. Rev. B **74**, 224445 (2006).

[14] P. Chaddah, K. Kumar, and A. Banerjee, Phys. Rev. B **77**, 100402(R) (2008).

[15] A. Banerjee, K. Kumar and P. Chaddah, J. Phys.: Condens. Matter **20**, 255245 (2008); **21**, 026002 (2009).

[16] S. B. Roy and M. K. Chattopadhyay, Phys. Rev. B **79**, 052407 (2009).

[17] S. Pal, K. Kumar, A. Banerjee, S. B. Roy, and A. K. Nigam, J. Phys.: Condens. Matter **33**, 025801 (2021).

[18] S. Pal, K. Kumar, R. Sharma, A. Banerjee, S. B. Roy, J.-G. Park, A. K. Nigam, and S.-W. Cheong, J. Phys.: Condens. Matter **32**, 035601 (2020).

[19] W. Wu, C. Israel, N. Hur, S. Park, S. W. Cheong, and A. De Lozanne, Nat. Mater. **5**, 881 (2006).

[20] Y. J. Choi, C. L. Zhang, N. Lee, and S.-W. Cheong, Phys. Rev. Lett. **105**, 097201 (2010)

[21] P. Saha and R. Rawat, Appl. Phys. Lett. **112**, 192409 (2018).

[22] B. Ghosh, D. K. Mahato, and S. Banerjee, Mater. Today: Proc. **5**, 15426 (2018).

[23] X. F. Miao, Y. Mitsui, A. Iulian Dugulan, L. Caron, N. V. Thang, P. Manuel, K. Koyama, K. Takahashi, N. H. van Dijk, and E. Bruck, Phys. Rev. B **94**, 094426 (2016).

[24] A. K. Nayak, M. Nicklas, C. Shekhar, and C. Felser, J. App. Phys. **113**, 17E308 (2013).

[25] D. J. Keavney, Y. Choi, M. V. Holt, V. Uhlíř, D. Arena, E. E. Fullerton, P. J. Ryan, and J. W. Kim, Sci. Report **8**, 1778 (2018).

[26] Ö. Çakır, E. Dias, K. R. Priolkar, A. Hoser, M. Farle, and M. Acet, Phys. Rev. B **102**, 024431 (2020).

[27] K. Matsuura *et al.*, Phys. Rev. B **103**, L041106 (2021).

[28] P. M. Chaikin and T. C. Lubensky, *Principles of Condensed Matter Physics* (Cambridge University Press, Cambridge, U.K, 1995).

[29] P. Chaddah, *First Order Phase Transition in Magnetic Materials: Broad and Interrupted Transitions* (CRC Press, Boca Raton, 2017).

[30] Y. Imry and M. Wortis, Phys. Rev. B **19**, 3580 (1979).

[31] K. Kumar, A. K. Pramanik, A. Banerjee, P. Chaddah, S. B. Roy, S. Park, C. L. Zhang, and S. W. Cheong, Phys. Rev. B **73**, 184435 (2006).

[32] A. Banerjee, A. K. Pramanik, K. Kumar, and P. Chaddah, J. Phys.: Condens. Matter **18**, L605 (2006).

[33] S. Nair and A. Banerjee, J. Phys.: Condens. Matter **16**, 8335 (2004).

[34] K. Mukherjee, K. Kumar, A. Banerjee, and P. Chaddah, Eur. Phys. J. B **86**, 21 (2013).

[35] A. K. Pramanik, R. Ranjan, and A. Banerjee, J. Magn. Magn. Mater. **325**, 29 (2013).

[36] S. Sharma, A. Shahee, P. Yadav, I. da Silva, and N. P. Lalla, J. Appl. Phys. **122**, 175902 (2017).

[37] V. Siriguri, P. D. Babu, S. D. Kaushik, A. Biswas, S. K. Sarkar, M. Krishnan, and P. Chaddah, J. Phys.: Condens. Matter **25**, 496011 (2013).

[38] A. N. Kolmogorov, Bull. Acad. Sci. U.S.S.R., Phys. Ser. **3**, 555 (1937); A. M. Johnson and R. F. Mehl, Trans. Am. Inst. Min. Metall. Pet. Eng. **135**, 417 (1939); M. Avarami, J. Chem. Phys. **7**, 212 (1940); **8**, 177 (1941)

[39] P. Levy, F. Parisi, L. Granja, E. Indelicato, and G. Polla, Phys. Rev. Lett. **89**, 137001 (2003).

[40] P. Levy, F. Parisi, M. Quintero, L. Granja, J. Curiale, J. Sacanell, G. Leyva, and G. Polla, Phys. Rev. B **65**, 140401(R) (2003).

[41] Y. T. Tsai, W. J. Chang, C. C. Hsieh, C. W. Luo, K. H. Wu, T. M. Uen, J. Y. Juang, and J. Y. Lin, J. App. Phys. **105**, 013705 (2009).

[42] H. T. Yi, T. Choi, and S. W. Cheong, App. Phys. Lett. **95**, 063509 (2009).

[43] T. Elovaara, H. Huhtinen, S. Majumdar, and P. Paturi, J. Phys.: Condens. Matter **24**, 216002 (2012).